H-infinity optimization of a variant design of the dynamic vibration absorber – revisited and new results

Y.L. Cheung and W.O. Wong
Department of Mechanical Engineering
The Hong Kong Polytechnic University, Hong Kong SAR, China

Abstract

The H_∞ optimum parameters of a dynamic vibration absorber (DVA) with ground-support are derived to minimize the resonant vibration amplitude of a single degree-of-freedom (SDOF) system under harmonic force excitation. The optimum parameters which are derived based on the classical fixed-points theory and reported in literature for this non-traditional DVA are shown to be not leading to the minimum resonant vibration amplitude of the controlled mass. A new procedure is proposed for the H_∞ optimization of such a dynamic vibration absorber. A new set of optimum tuning frequency and damping of the absorber is derived, thereby resulting in lower maximum amplitude responses than those reported in the literature. The proposed optimized variant DVA is also compared to a ground-hooked damper of the same damping capacity of the damper in the DVA. It is proved that the proposed optimized DVA has better suppression of the resonant vibration amplitude of the controlled system than both the traditional DVA and also the ground-hooked damper if the proposed design procedure of the variant DVA is followed.

Keywords: vibration absorber; fixed-points theory; optimization

1. Introduction

The traditional dynamic vibration absorber is an auxiliary mass-spring system which, when correctly tuned and attached to a vibrating system subject to harmonic excitation,

causes to cease the steady-state motion at the point to which it is attached [1]. It has the advantage of providing a cheap and easy-to-maintain solution for suppressing vibration in vibrating systems with harmonic excitation. The traditional DVA is found to be very useful in the fields of civil and mechanical engineering because of its simple design and high reliability. A damper is often added between the absorber mass m and the primary mass M as illustrated in Fig. 1 to limit the vibration amplitude when the lower resonance is experienced during system startup and stopping. However, it is not possible to eliminate steady-state vibrations of the original mass after damping is added to the auxiliary mass-spring system [1].

Considerable research work has been carried out in deriving analytically the optimum parameters [1-4] of the traditional DVA when it is applied to a single degree-of-freedom (SDOF) primary system. In 1928, Ormondroyd and Den Hartog [1] pointed out that the damping of the DVA had an optimum value for the minimization of the resonance amplitude magnification factor of a SDOF system. Such optimization criterion is now known as H_∞ optimization. Brock [2] derived the optimum damping and Hahnkamm [3] deduced the optimum tuning frequency of the traditional DVA. This optimum design method of the dynamic vibration absorber is based on the famous "fixed-points theory" [4] which says that all frequency response curves pass through two invariant points independent of the absorber damping. The fixed-points theory is the earliest method found in literature applied to solve analytically for the optimum parameters of the traditional DVA for the undamped SDOF primary system as illustrated in Fig. 1. The optimal tuning frequency and damping ratios of the traditional DVA derived using the fixed-points theory are not exact because some approximations are taken when they are derived [3,4]. Nishihara and Asami [5] derived the exact H_∞ frequency and damping ratios of the traditional DVA using another method and compared the ratios to those proposed by Den

Hartog [4]. Nishihara and Asami reported that both the optimal frequency and damping ratios proposed by Den Hartog were very close to the exact values. The differences between the optimal [4] and the exact [5] frequency and damping ratios were less than 1% and 2% respectively when the mass ratio was less than 0.5. Therefore, the optimal frequency and damping ratios of the DVA derived using the fixed-points theory did provide a very good approximation of the exact H_∞ optimal frequency and damping ratios.

In the last few years, the fixed-points theory has been extended for the optimization of the traditional DVA applied to multi-DOF [6] and continuous [7,8,9] primary systems. The fixed-points theory has also been used in deriving the optimum parameters of a tuned liquid column damper for suppressing harmonic vibration of structures [10]. A perturbation method is proposed by Asami et al. [11] for deriving the H_∞ optimum parameters of a damped DVA applied to a damped SDOF primary system. Their proposed analytical expressions for the optimum tuning frequency and damping ratio of the traditional DVA are very long and complicated and they may not be easily applied in practice.

A variant design of the damped dynamic vibration absorber as shown in Fig. 2 was proposed by Ren [12], and Liu and Liu [13] recently and this non-traditional DVA would be useful in some applications [14]. Based on the fixed-points theory, the optimum tuning parameters of such a vibration absorber had been derived analytically for minimizing the resonant vibration of a SDOF system subjected to force excitation [12-14] or caused by ground motions [15]. The optimized non-traditional absorber was shown to have resulted in a larger reduction of the resonant vibration amplitude of the primary mass than the traditional damped dynamic absorber. In Section 3 it is shown that for this non-traditional DVA the optimum tuning parameters derived by the fixed-points theory does not lead to the minimum resonant amplitude of a SDOF system subjected to

harmonic force excitation. A new procedure is proposed for the H_∞ optimization of such a non-traditional dynamic vibration absorber. A new set of optimum tuning frequency and damping ratios of the absorber is derived, thereby resulting in lower maximum amplitude responses than those responses found in the literature [12,13].

2. The traditional damped dynamic vibration absorber

A schematic diagram of a traditional damped dynamic vibration absorber attached to an undamped mass-spring system is shown in Fig. 1. This vibration model is called model A in the following discussion. The amplitude ratio $|X_1/X_{st}|_A$ given by Den Hartog [1] is:

$$|G_A(\lambda)| = \left|\frac{X_1}{X_{st}}\right|_A$$

$$= \sqrt{\frac{\left(\gamma^2-\lambda^2\right)^2+(2\zeta\gamma\lambda)^2}{\left[\left(1-\lambda^2\right)\left(\gamma^2-\lambda^2\right)-\mu\gamma^2\lambda^2\right]^2+(2\zeta\gamma\lambda)^2\left(1-\mu\lambda^2-\lambda^2\right)^2}}\,. \tag{1}$$

where $X_{st} = F/K$, $\lambda = \omega/\sqrt{K/M}$, $\gamma = \sqrt{k/m}/\sqrt{K/M}$, $\mu = m/M$, and $\zeta = c/2\sqrt{mk}$.

In the H_∞ optimization, the objective function is to minimize the maximum amplitude ratio of the response of the primary system to the excitation force, i.e.

$$\max\left(\left|G_A\left(\lambda,\gamma_{opt\_A},\zeta_{opt\_A}\right)\right|\right) = \min\left(\max_{\gamma,\zeta}\left|G_A(\lambda)\right|\right). \tag{2}$$

The procedure in deriving the optimum tuning frequency and damping ratios of the absorber based on the fixed-points theory by Den Hartog [4] to minimize the maximum amplitude ratio of the response of the primary system is briefly described in the following.

For the purpose of illustration, frequency response curves of the primary mass M, $|G_A(\lambda)|$, of the traditional vibration absorber (Fig. 1) with $\mu = 0.1$, $\gamma = 1$ and $\zeta = 0.01$, 0.2 and 0.5 are calculated using Eq. (1) and the results are plotted in Fig. 3. The intersecting points P and Q in Fig. 3 are independent of the damping ratio ζ and they are

called “fixed points”. The dimensionless frequencies of the points P and Q are [1]

$$\lambda_{P,Q} = \sqrt{\frac{1+\gamma^2+\mu\gamma^2 \mp \sqrt{1-2\gamma^2+(1+\mu)^2\gamma^4}}{2+\mu}} \,. \tag{3}$$

The amplitudes of the frequency response at λ_P and λ_Q are [1]

$$\left|G_{\mathrm{A}}(\lambda_P)\right| = \left|\frac{1}{1-\lambda_P^2-\mu\lambda_P^2}\right| = \frac{2+\mu}{1-\gamma^2(1+\mu)^2+(1+\mu)\sqrt{1-2\gamma^2+\gamma^4(1+\mu)^2}} \tag{4a}$$

and

$$\left|G_{\mathrm{A}}(\lambda_Q)\right| = \left|\frac{1}{1-\lambda_Q^2-\mu\lambda_Q^2}\right| = -\frac{2+\mu}{1-\gamma^2(1+\mu)^2-(1+\mu)\sqrt{1-2\gamma^2+\gamma^4(1+\mu)^2}} \,. \tag{4b}$$

At any damping ratio, the frequency response must pass through these two fixed points P and Q. Eqs. (4a) and (4b) are calculated with μ = 0.2 and the response magnitude $\left|G_{\mathrm{A}}(\lambda_P)\right|$ and $\left|G_{\mathrm{A}}(\lambda_Q)\right|$ of mass M at the two fixed points are plotted in Fig. 4a for illustration, the curves $\left|G_{\mathrm{A}}(\lambda_P)\right|$ and $\left|G_{\mathrm{A}}(\lambda_Q)\right|$ have an intersection point indicating that there is a tuning frequency of the absorber at which the two response magnitude are the same. Den Hartog [4] considered this frequency parameter to be the optimum tuning frequency parameter of the vibration absorber. This tuning frequency is written as [4]

$$\gamma_{\mathrm{opt\_A}} = \frac{1}{1+\mu} \,. \tag{5}$$

As shown in Fig. 4b, the response magnitude at this intersection point is the global minimum of the function $\max\left(\left|G_{\mathrm{A}}(\lambda_P)\right|,\left|G_{\mathrm{A}}(\lambda_Q)\right|\right)$ and the response magnitude at either point P or Q will be higher than this minimum at any other tuning frequency. To determine the optimum damping of the absorber in order to make points P and Q the maximum points on the response curve, zero slope is considered at the two stationary points P and Q, i.e.

$$\frac{\partial}{\partial \lambda}\left(\left|G_{\mathrm{A}}(\lambda)\right|\right)^2 = 0 . \tag{6}$$

It can be shown that [4] there are two separate damping values that causes zero slopes at fixed-points P and Q separately, the optimal damping value is chosen to be the average of these two damping values for convenience and it can be derived and written as [4]

$$\zeta_{\mathrm{opt\_A}} = \sqrt{\frac{3\mu}{8(1+\mu)}} . \tag{7}$$

An approximate value of the amplitude ratio at resonance derived by Den Hartog [4] is

$$\left|\frac{X_1}{X_{\mathrm{st}}}\right|_{\mathrm{max\_A}} = \sqrt{\frac{2+\mu}{\mu}} . \tag{8}$$

Eq. (8) above shows that the maximum amplitude ratio $|X_1/X_{\mathrm{st}}|_{\mathrm{max\_A}}$ must be larger than one and it approaches one when the mass ratio μ approaches infinity. In practice, seldom would μ be larger than 0.25 [16] and therefore the resonant vibration amplitude of M is at least three times the static deflection, X_{st}.

3. A variant form of the damped dynamic vibration absorber

A variant form of the damped dynamic vibration absorber as shown in Fig. 2 was proposed recently [12,13]. This is called model B in the following discussion. The amplitude ratio $|X_1/X_{\mathrm{st}}|_{\mathrm{B}}$ derived using the fixed-points theory by Ren [12] is:

$$\begin{aligned}\left|G_{\mathrm{B}}(\lambda)\right| &= \left|\frac{X_1}{X_{\mathrm{st}}}\right|_{\mathrm{B}} \\ &= \sqrt{\frac{\left(\gamma^2-\lambda^2\right)^2+(2\zeta\gamma\lambda)^2}{\left[\left(1-\lambda^2\right)\left(\gamma^2-\lambda^2\right)-\mu\gamma^2\lambda^2\right]^2+(2\zeta\gamma\lambda)^2\left(1+\mu\gamma^2-\lambda^2\right)^2}} .\end{aligned} \tag{9}$$

In the H_∞ optimization, the objective function is to minimize the maximum amplitude ratio of the response of the primary system to the excitation, i.e.

$$\max\left(\left|G_{\mathrm{B}}\left(\lambda,\gamma_{\mathrm{opt\_B}},\zeta_{\mathrm{opt\_B}}\right)\right|\right)=\min\left(\max_{\gamma,\zeta}\left|G_{\mathrm{B}}\left(\lambda\right)\right|\right). \tag{10}$$

Eq. (9) may be rewritten into the form as

$$\left|G_{\mathrm{B}}\left(\lambda\right)\right|=\sqrt{\frac{A+B\zeta^2}{C+D\zeta^2}} \tag{11}$$

where $A=\left(\gamma^2-\lambda^2\right)^2$, $B=\left(2\gamma\lambda\right)^2$, $C=\left[\left(1-\lambda^2\right)\left(\gamma^2-\lambda^2\right)-\mu\lambda^2\gamma^2\right]^2$, and $D=\left(2\gamma\lambda\left(1-\lambda^2+\mu\gamma^2\right)\right)^2$.

Frequency responses of the primary mass *M* are calculated according to Eq. (9) with three damping ratios and the results are shown in Fig. 5. It is noted that there are intersecting points *O*, *P* and *Q*, which are independent of the absorber damping. Substituting $\lambda=0$ into Eq. (9) always leads to amplitude ratio $G_{\mathrm{B}}\left(0\right)=1$ and it corresponds to the fixed point *O* in Fig. 5. To find the other fixed points *P* and *Q*, we consider the frequency response curves for $\zeta=0$ and $\zeta=\infty$. Since both frequency response curves for $\zeta=0$ and $\zeta=\infty$ would pass through fixed points *P* and *Q*, we may write

$$\frac{A}{C}=\frac{B}{D}. \tag{12}$$

Noting that $\lambda_P\neq0$ and $\lambda_Q\neq0$, Eq. (12) may be simplified as

$$\left(\frac{\gamma^2-\lambda^2}{\left(1-\lambda^2\right)\left(\gamma^2-\lambda^2\right)-\mu\lambda^2\gamma^2}\right)^2=\left(\frac{1}{1-\lambda^2+\mu\gamma^2}\right)^2. \tag{13}$$

Taking square root on both sides of Eq. (13), we have

$$\frac{\gamma^2-\lambda^2}{\left(1-\lambda^2\right)\left(\gamma^2-\lambda^2\right)-\mu\lambda^2\gamma^2}=\pm\frac{1}{1-\lambda^2+\mu\gamma^2}. \tag{14}$$

Noting that the responses at $\zeta=0$ and $\zeta=\infty$ are in opposite phases, negative sign on the right hand side of Eq. (14) is therefore taken and we may write

$$\frac{\gamma^2-\lambda^2}{\left(1-\lambda^2\right)\left(\gamma^2-\lambda^2\right)-\mu\lambda^2\gamma^2}=-\frac{1}{1-\lambda^2+\mu\gamma^2}. \tag{15}$$

Eq. (15) may be rewritten as

$$2\lambda^4 - 2\left(1+\gamma^2+\mu\gamma^2\right)\lambda^2 + 2\gamma^2 + \mu\gamma^4 = 0\,. \tag{16}$$

The roots of Eq. (16) are λ_{P} and λ_{Q} and they are written as

$$\lambda_{P,Q} = \sqrt{\frac{1+\gamma^2+\mu\gamma^2 \mp \sqrt{1-2(1-\mu)\gamma^2+\left(1+\mu^2\right)\gamma^4}}{2}}\,. \tag{17}$$

The amplitudes of the frequency response at these two roots are independent of the damping ratio ζ and they are written as

$$\left|G_{\mathrm{B}}(\lambda_P)\right| = \left|\frac{1}{1-\lambda_P^2+\mu\gamma^2}\right| = \frac{2}{1-\gamma^2+\mu\gamma^2+\sqrt{1-2(1-\mu)\gamma^2+\left(1+\mu^2\right)\gamma^4}}\text{, and} \tag{18}$$

$$\left|G_{\mathrm{B}}(\lambda_Q)\right| = \left|\frac{1}{1-\lambda_Q^2+\mu\gamma^2}\right| = -\frac{2}{1-\gamma^2+\mu\gamma^2-\sqrt{1-2(1-\mu)\gamma^2+\left(1+\mu^2\right)\gamma^4}}\,. \tag{19}$$

At any damping ratio, the frequency response must include these three fixed points *O*, *P* and *Q*. The H_∞ optimization of the variant design of DVA may be restated as:

If the function $\left|G_{\mathrm{B}}(\gamma,\zeta,\lambda)\right|$ has any point S_n which is independent of the variable ζ and the response amplitude at S_n is a global maximum of $\left|G_{\mathrm{B}}(\lambda)\right|$ for $\forall\lambda\in R^+$, γ is the optimal tuning frequency and ζ is the optimal damping.

$\left|G_{\mathrm{B}}(\lambda_P)\right|$ and $\left|G_{\mathrm{B}}(\lambda_Q)\right|$ are calculated according to Eqs. (18) and (19) with μ = 0.1 and they are plotted together with $\left|G_{\mathrm{B}}(\lambda_0)\right|$ in Fig. 6a for illustration. $\left|G_{\mathrm{B}}(\lambda_P)\right|$ and $\left|G_{\mathrm{B}}(\lambda_Q)\right|$ has an intersection point *R* in Fig. 6a. By solving $\left|G_{\mathrm{B}}(\lambda_P)\right|=\left|G_{\mathrm{B}}(\lambda_Q)\right|$, the tuning frequency at this intersection point can be found and written as [12,13]

$$\gamma_R = \sqrt{\frac{1}{1-\mu}}\,. \tag{20}$$

It can be shown that [12] there are two separate damping values that causes zero slopes of $\left|G_{\mathrm{B}}(\lambda)\right|$ at fixed-points *P* and *Q* separately and the optimal damping value is chosen to be

the average of these two damping values for convenience it can be written as [12]

$$\zeta_R = \sqrt{\frac{3\mu}{8(1-0.5\mu)}}. \tag{21}$$

The tuning frequency γ_R and damping ζ_R were considered to be the optimum tuning frequency and damping of the absorber by Ren [12], and Liu and Liu [13]. An approximate value of the dimensionless resonant vibration amplitude of mass *M* is derived and written as (Eq. (12) of [12], and Eq. (12) of [13])

$$\left|\frac{X_1}{X_{st}}\right|_{\max\_B} = (1-\mu)\sqrt{\frac{2}{\mu}}. \tag{22}$$

As shown in Fig. 6b, there is a point *S* on the curve of $|G_B(\lambda_P)|$ where $|G_B(\gamma_R, \lambda_P)| = |G_B(\gamma_S, \lambda_P)|$. Using equations (18) and (22), consider $|G_B(\lambda_P)| = \left|\frac{X_1}{X_{st}}\right|_{\max\_B}$, the tuning ratio γ_S at point *S* in Fig. 7b can be solved and written as

$$\gamma_S = \sqrt{\frac{(\sqrt{2}+\sqrt{\mu})(1-\sqrt{2\mu})}{\sqrt{\mu}(1-\mu)}} \tag{23}$$

As shown in Fig. 6b, point *R* is a local minimum point but point *T* is the global minimum of $\max_{\gamma,\zeta}(|G_B(\lambda_P)|, |G_B(\lambda_Q)|, |G_B(\lambda_o)|)$. Theoretically, the dimensionless resonant vibration amplitude of mass *M*, can be reduced to one if the tuning frequency at point *T* instead of point *R* is chosen. The tuning ratio γ_T is found by solving $G_B(\lambda_P) = 1$ and written as

$$\gamma_T = \sqrt{\frac{2(1-\mu)}{\mu}} \tag{24}$$

However, γ_T may be too high to be applied in practice and the following practical constraints are assumed in the design formulation of the vibration system:

$$0 < \mu \le 0.25, \tag{25a}$$

$$k \le K, \text{ and} \tag{25b}$$

$$\zeta_{\text{opt\_B}} \le 1. \tag{25c}$$

The tuning frequency of the DVA may be rewritten as

$$\gamma = \sqrt{\frac{k}{K\mu}}\,. \tag{26}$$

Assuming the practical constraints of $k \le K$ and $\mu \le 0.25$, we may consider a practical range of the optimum tuning frequency parameter of model B using Eq. (26) written as

$$\gamma_{\mathrm{S}} \le \gamma_{\mathrm{opt\_B}} \le \sqrt{\frac{1}{\mu}}\,,\quad 0 < \mu \le 0.25\,. \tag{27}$$

To determine the optimum damping of the absorber in order to make point P to be the maximum point on the response curve, it requires zero slope at the stationary point P, i.e.

$$\frac{\partial}{\partial\lambda}\left|G_{\mathrm{B}}(\lambda)\right|^2\Big|_{\lambda=\lambda_P} = 0\,. \tag{28}$$

Using Eqs. (9), (17) and (28), the optimum damping can be derived and written as

$$\zeta_{\mathrm{opt\_B}} = \sqrt{\frac{1-2\gamma^2(1-\mu)+\gamma^4\left(1+\mu+\mu^2\right)-\left(1-\gamma^2(1-\mu)\right)\sqrt{1-2(1-\mu)\gamma^2+\left(1+\mu^2\right)\gamma^4}}{4\gamma^2\left(1+\gamma^2+\mu\gamma^2-\sqrt{1-2(1-\mu)\gamma^2+\left(1+\mu^2\right)\gamma^4}\right)}}\,. \tag{29}$$

The maximum frequency response of the primary structure of model B may be written as

$$\max\left(\left|G_{\mathrm{B}}\left(\lambda,\mu,\gamma_{\mathrm{opt\_B}},\zeta_{\mathrm{opt\_B}}\right)\right|\right) = \left|G_{\mathrm{B}}\left(\lambda_P\right)\right| = \frac{2}{1-\gamma^2+\mu\gamma^2+\sqrt{1-2(1-\mu)\gamma^2+\left(1+\mu^2\right)\gamma^4}} \tag{30}$$

It is proved that the intersection point R between $\left|G_{\mathrm{B}}(\lambda_P)\right|$ and $\left|G_{\mathrm{B}}(\lambda_Q)\right|$ is a local minimum only when $0 \le \mu < 2-\sqrt{3}$ and the derivation is shown in the Appendix. As shown in Fig. 6b, the response magnitude at this intersection point is the local minimum of the function $\max\left(\left|G_{\mathrm{B}}(\lambda_P)\right|,\left|G_{\mathrm{B}}(\lambda_Q)\right|\right)$ and the response magnitude at either point P or Q will be higher than this minimum at any other tuning frequency in the range of $0 \le \mu < 2-\sqrt{3}$. $\left|G_{\mathrm{B}}(\lambda_P)\right|$ and $\left|G_{\mathrm{B}}(\lambda_Q)\right|$ are calculated according to Eqs. (18) and (19) respectively with $\mu = 2-\sqrt{3}$ and they are plotted together with $\left|G_{\mathrm{B}}(\lambda_o)\right|$ in Fig. 7a for

illustration. $|G_{\mathrm{B}}(\lambda_P)|$ and $|G_{\mathrm{B}}(\lambda_Q)|$ has an intersection point R at the peak of the curve of $|G_{\mathrm{B}}(\lambda_P)|$as shown in Fig. 7a. The point R is not a local minimum of the function $\max\left(|G_{\mathrm{B}}(\lambda_P)|,|G_{\mathrm{B}}(\lambda_Q)|\right)$ anymore. As shown in Fig. 7b, when $\mu = 2-\sqrt{3} = 0.2679$, both the response amplitude $|G_{\mathrm{B}}(\lambda_P)|$ and $|G_{\mathrm{B}}(\lambda_Q)|$ decrease when γ increases beyond γ_R and therefore the resonant amplitude would reduce if the tuning frequency parameter of the DVA, γ is chosen to have a value larger than γ_R. This means that the optimum tuning frequency and damping ratios of the absorber proposed by Ren [12], and Liu and Liu [13] based on the fixed-points theory are only valid in the range of $0 \le \mu \le 2-\sqrt{3}$. Their proposed optimum tuning frequency and damping ratios as shown in Eqs. (20) and (21) respectively would still lead to double equal peaks in the response spectrum $|G_{\mathrm{B}}(\lambda)|$ when $\mu > 2-\sqrt{3}$ but the maximum response amplitude of the mass *M* will decrease if the frequency parameter γ is increased from γ_R.

Frequency response curves of the primary mass *M* of the non-traditional vibration absorber based on the two sets of optimum tuning frequency and damping ratios, one applying the fixed-points theory (Eqs. 20 and 21) and the other using the present theory (Eqs. 27 and 29) are calculated according to Eq. (9) and the results are plotted with the dotted and solid lines respectively in Fig. 8 for comparison. Mass ratio μ is chosen to be 0.25 for the purpose of illustration. The curve generated based on the fixed-points theory shows the standard double peak characteristic but its resonant peaks are found to be 63% higher than the peaks of the second curve generated based on the present theory. The frequency response curve using γ_T and $\zeta_T = \zeta_{\mathrm{opt\_B}}\big|_{\gamma=\gamma_T}$ is also calculated and plotted as the centerline in Fig. 8 for illustration. The dimensionless resonant amplitude becomes one but the stiffness *k* and damping *c* of the DVA are high in this case and therefore it is assumed that γ_T and ζ_T cannot be applied in practice.

Since the proposed DVA has its damper connected to the ground, it is also compared to the

case that the damper connected directly between the primary mass and the ground without using the absorber system as illustrated in Fig. 9 and it is called model C in the following discussion. To compare the resonant vibration amplitude of the mass *M* of model B to that of model C, the frequency response of the primary mass *M* of model B in Eq. (9) is rewritten as

$$|G_{\mathrm{B}}(\lambda)| = \left|\frac{X_1}{X_{\mathrm{st}}}\right|_{\mathrm{B}} = \sqrt{\frac{\mu^2\left(\gamma^2-\lambda^2\right)^2+(2\zeta'\lambda)^2}{\mu^2\left[\left(1-\lambda^2\right)\left(\gamma^2-\lambda^2\right)-\mu\gamma^2\lambda^2\right]^2+(2\zeta'\lambda)^2\left(1+\mu\gamma^2-\lambda^2\right)^2}} \tag{31}$$

where $\zeta' = \dfrac{c}{2\sqrt{MK}} = \mu\gamma\zeta$.

The optimum damping of model B may be rewritten using Eq. (29) as

$$\zeta'_{\mathrm{opt\_B}} = \mu\gamma\zeta_{\mathrm{opt\_B}}$$

$$= \mu\sqrt{\frac{1-2\gamma^2(1-\mu)+\gamma^4\left(1+\mu+\mu^2\right)-\left(1-\gamma^2(1-\mu)\right)\sqrt{1-2(1-\mu)\gamma^2+\left(1+\mu^2\right)\gamma^4}}{4\left(1+\gamma^2+\mu\gamma^2-\sqrt{1-2(1-\mu)\gamma^2+\left(1+\mu^2\right)\gamma^4}\right)}} \tag{32}$$

Assuming that the damper of model C has the optimum damping of model B, the frequency response of the primary mass *M* of model C may be written as

$$|G_{\mathrm{C}}(\lambda)| = \left|\frac{X_1}{X_{\mathrm{st}}}\right|_{\mathrm{C}} = \sqrt{\frac{1}{\left(1-\lambda^2\right)^2+\left(2\zeta'_{\mathrm{opt\_B}}\lambda\right)^2}} \tag{33}$$

The resonant frequency of model C can be found to be $\lambda = \sqrt{1-2(\zeta'_{\mathrm{opt\_B}})^2}$ by considering $\dfrac{\partial}{\partial\lambda}|G_{\mathrm{C}}(\lambda)|^2 = 0$. The resonant vibration amplitude of model C can then be found by substituting $\lambda = \sqrt{1-2(\zeta'_{\mathrm{opt\_B}})^2}$ into Eq. (33) and written as

$$\max(|G_{\mathrm{C}}(\lambda)|) = \frac{1}{2\zeta'_{\mathrm{opt\_B}}\sqrt{1-(\zeta'_{\mathrm{opt\_B}})^2}} \tag{34}$$

To compare the resonant vibration amplitude of model B to model C at different mass ratio μ and frequency parameter γ of the DVA of model B, the resonant vibration amplitude

of Model C, $\max(|G_{\mathrm{C}}(\lambda)|)$, is calculated according Eq. (34) and the damping ratio $\zeta'_{\mathrm{opt\_B}}$ is calculated according to Eq. (32) such that both model B and model C have dampers of same damping coefficient *c*. The resonant vibration amplitude of model B, $\max\left(\left|G_{\mathrm{B}}\left(\lambda,\mu,\gamma_{\mathrm{opt\_B}},\zeta_{\mathrm{opt\_B}}\right)\right|\right)$, is calculated according Eq. (30) and the percentage differences at different mass ratio and frequency between $\max(|G_{\mathrm{C}}(\lambda)|)$ and $\max\left(\left|G_{\mathrm{B}}\left(\lambda,\mu,\gamma_{\mathrm{opt\_B}},\zeta_{\mathrm{opt\_B}}\right)\right|\right)$ are plotted in Fig. 10. The zero contour in Fig. 10 represents the curve of $\max(|G_{\mathrm{C}}(\lambda)|) = \max\left(\left|G_{\mathrm{B}}\left(\lambda,\mu,\gamma_{\mathrm{opt}},\zeta_{\mathrm{opt}}\right)\right|\right)$. As shown by the region of the positive contours in Fig. 10, the resonant vibration amplitude of the primary mass *M* using the variant DVA is found to be better than using the damper alone in the range of $\mu \le 0.22$ with the frequency parameter γ of the DVA less than 1.82 and in the range of $\mu > 0.22$ with any positive value of γ. The zero contour in Fig. 10 is plotted as dotted line together with the contours of $\max\left(\left|G_{\mathrm{B}}\left(\lambda,\mu,\gamma_{\mathrm{opt}},\zeta_{\mathrm{opt}}\right)\right|\right)$ in Fig. 11. The curve of γ_S at different mass ratio μ is calculated according to Eq. (23) and plotted as centerline in Fig. 11. There is an intersection of the curve of γ_S and the dotted line representing $\max(|G_{\mathrm{C}}(\lambda)|) = \max\left(\left|G_{\mathrm{B}}\left(\lambda,\mu,\gamma_{\mathrm{opt}},\zeta_{\mathrm{opt}}\right)\right|\right)$ in Fig. 11. This intersection appears at frequency parameter $\gamma = 1.89$ and mass ratio $\mu = 0.092$. According to Eq. (27), $\gamma_{\mathrm{opt\_B}}$ should be chosen to be larger than γ_{S} so that the resonant vibration amplitude $\max\left(\left|G_{\mathrm{B}}(\lambda)\right|\right)$ using the proposed tuning parameters is smaller than that using the values proposed in Refs. [12] and [13], i.e. $\gamma = \gamma_R$ and $\zeta = \zeta_R$. Therefore, the resonant vibration amplitude of the primary mass *M* using the variant DVA is found to be better than just using the damper alone when $0.092 < \mu < 0.22$ with the frequency parameter γ of value smaller than those on the dotted curve in Fig. 11. When $\mu > 0.22$, the resonant vibration amplitude of the primary mass *M* using a variant DVA is always better than just

using the damper alone. A convenient formula of the optimum tuning frequency parameter of the non-traditional DVA is proposed as

$$\gamma_{\text{opt\_B}} \begin{cases} = 2.02 - 1.5\mu & 0.092 < \mu \le 0.22 \\ \le \sqrt{\frac{1}{\mu}} & 0.22 < \mu < 0.25 \end{cases} \tag{35}$$

$\gamma_{\text{opt\_B}}$ is chosen according to Eq. (35) to ensure the proposed absorber will perform better than the traditional DVA and the primary damper alone. The comparison is shown in Fig. 12. In Fig. 12, the resonant vibration amplitude $\max\left(\left|G_{\text{B}}(\lambda)\right|\right)$ of the mass M of Model B at different mass ratio are calculated according to Eq. (30) with the proposed optimum tuning parameters $\gamma = \gamma_{\text{opt\_B}}$ and $\zeta = \zeta_{\text{opt\_B}}$ and compared to the one using the optimum tuning parameters $\gamma = \gamma_R$ and $\zeta = \zeta_R$ proposed in Refs. [12] and [13]. It is also compared to the case with the damper of damper coefficient c attached directly between the primary mass M and the ground. It is found that the resonant vibration amplitude $\max\left(\left|G_{\text{B}}(\lambda)\right|\right)$ using the proposed tuning parameters is always smaller than that using the values proposed in Refs. [12] and [13] and also smaller than just using the damper alone if $\mu > 0.092$. The reduction of maximum response amplitude of the primary mass M in model B using the proposed optimal parameters increases from 2.5% to 21% more than that using the values proposed in Refs. [12] and [13] and increases from 1.6% to 18% more than just using the damper alone when the mass ratio μ increases from 0.1 to 0.25.

4. Conclusion

The fixed-points theory commonly used in the optimization of dynamic vibration absorber (DVA) is reviewed. It is found that the optimum parameters of the non-traditional DVA as shown in Fig. 2 reported in literature using the fixed-points theory may not lead to the minimization of the maximum amplitude magnification factor of the primary system. A new procedure is proposed for the H_∞ optimization of such a dynamic vibration absorber and a new set of optimum tuning frequency and damping of the absorber is derived, thereby resulting in a lower maximum amplitude response than the response reported in the literature [12,13]. The new optimum tuning frequency

parameter proposed for the H_∞ optimization of such a dynamic vibration absorber is given in Eq. (35) and the corresponding damping ratio of the absorber is given in Eq. (29).

Fig. 11 may be used in practice for choosing the set of mass ratio and frequency parameter of the variant DVA for the desired resonant vibration amplitude of the primary mass and this resonant vibration amplitude is smaller than the one using the optimum values proposed by other researchers [12, 13] and also better than the one using the damper alone in the range of mass ratio $\mu \geq 0.092$. The conventional wisdom of suppressing vibration of a machine is to add a damper to its mounting or a traditional DVA if the added structure cannot be mounted onto the ground. We have proved that the proposed variant DVA with ground-support has better suppression of the resonant vibration amplitude than the traditional DVA and also the damper alone. For example, if a machine has a large vibration at resonance and the engineer plans to add an absorber or a damper to reduce its vibration at resonance. The additional structure may be designed rather freely, and there is an optional ground-support. We provided an additional option and design guidelines to the engineer to apply the proposed DVA with ground-support for suppressing the resonant vibration of the machine.

The optimum tuning frequency and damping ratios proposed are derived only for the H_∞ optimization of model B and the resonant vibration amplitude of the primary mass is less than the one using the damper alone (model C). The H_2 optimization of model B would require another set of optimum tuning frequency and damping ratios. Since the derivation of the H_2 optimal parameters of the variant DVA is very different from the present case and the comparison result of the effectiveness of the models B and C are found to be quite different from the result of the present case, the H_2 optimization of model B will be reported elsewhere.

Acknowledgement

The authors wish to acknowledge support given to them by the Central Research Grant of The Hong Kong Polytechnic University. The authors also acknowledge the reviewers as they raised some fundamental questions about the original theme of the paper and the final version of this paper has benefited from the review process.

Appendix

Referring to Fig. 7, point R is the maximum of $|G_{\mathrm{B}}(\lambda_P)|$ and it satisfies the condition $\frac{\partial|G_{\mathrm{B}}(\lambda_P)|}{\partial\gamma^2}=0$.

where $|G_{\mathrm{B}}(\lambda_P)|$ is given in Eq. (18).

$$\frac{\partial|G_{\mathrm{B}}(\lambda_P)|}{\partial\gamma^2}=-2\frac{-1+\mu+\dfrac{\mu-1+(\mu^2+1)\gamma^2}{\sqrt{1-2(1-\mu)\gamma^2+(1+\mu^2)\gamma^4}}}{\left(1-\gamma^2+\mu\gamma^2+\sqrt{1-2(1-\mu)\gamma^2+(1+\mu^2)\gamma^4}\right)^2}=0 \tag{A1}$$

$$\Rightarrow(1-\mu)\sqrt{1+2(\mu-1)\gamma^2+(\mu^2+1)\gamma^4}=\mu-1+(\mu^2+1)\gamma^2. \tag{A2}$$

Point R is also the intersection point of curves $|G_{\mathrm{B}}(\lambda_P)|$ and $|G_{\mathrm{B}}(\lambda_Q)|$ and therefore the corresponding γ at point R equals to γ_R and is expressed in Eq. (20). Substituting Eq. (20) into Eq. (A2), we may write

$$\sqrt{-1+\frac{\mu^2+1}{(1-\mu)^2}}=-1+\frac{\mu^2+1}{(1-\mu)^2} \tag{A3}$$

$$\Rightarrow\mu^2-4\mu+1=0 \tag{A4}$$

$$\Rightarrow\mu=2-\sqrt{3}\ \text{ or }\ \mu=\tfrac{1}{2-\sqrt{3}}\ (\text{discarded because }\ \mu>1). \tag{A5}$$

So mass ratio $\mu=2-\sqrt{3}$ when the intersection point of curves $|G_{\mathrm{B}}(\lambda_P)|$ and $|G_{\mathrm{B}}(\lambda_Q)|$ becomes also the maximum of $|G_B(\lambda_P)|$ as shown in Fig. 7.

References

[1] J. Ormondroyd and J. P. Den Hartog, The theory of the dynamic vibration absorber, *Journal of Applied Mechanics* 50 (1928) 9-22.

[2] J. E. Brock, A note on the damped vibration absorber, *Journal of Applied Mechanics* 13 (1946) A-284.

[3] E. Hahnkamm, Die Dampfung von Fundamentschwingungen bei veranderlicher Erregerfrequenz, *Ingenieur Archiv* 4 (1932) 192-201, (in German).

[4] J. P. Den Hartog, *Mechanical Vibrations*, Dover Publications Inc., 1985.

[5] O. Nishihara and T. Asami, Closed-Form Solutions to the Exact Optimizations of Dynamic Vibration Absorbers (Minimizations of the Maximum Amplitude Magnification Factors), *Journal of Vibration and Acoustics* 124 (2002) 576 – 582.

[6] M. B. Ozer, and T. J. Royston, Extending Den Hartog's Vibration Absorber Technique to Multi-Degree-of-Freedom Systems, *ASME Journal of Vibration and Acoustics* 127 (2005) 341–350.

[7] J. Dayou, Fixed-points theory for global vibration control using vibration neutralizer, *Journal of Sound and Vibration* 292 (2006) 765 – 776.

[8] J. Dayou and S. Wang, Derivation of the fixed-points theory with some numerical simulations for global vibration control of structure with closely spaced natural frequencies, *Mechanics based Design of Structures and Machines* 34 (2006) 49-68.

[9] Y. L. Cheung and W. O. Wong, H_∞ and H_2 optimizations of dynamic vibration absorber for suppressing vibrations in plates, *Journal of Sound and Vibration* 320 (2009) 29-42.

[10] K. M. Shum, Closed form optimal solution of a tuned liquid column damper for suppressing harmonic vibration of structures, *Engineering Structures* 31 (2009) 84-92.

[11] T. Asami, O. Nishihara and A.M. Baz, Analytical Solutions to H_∞ and H_2 Optimization of Dynamic Vibration Absorbers Attached to Damped Linear Systems, *Journal of Vibration and Acoustics* 124 (2002) 284 – 295.

[12] M. Z. Ren, A variant design of the dynamic vibration absorber, *Journal of Sound and Vibration* 245 (2001) 762-770.

[13] K. Liu and J. Liu, The damped dynamic vibration absorbers: revisited and new result, *Journal of Sound and Vibration* 284 (2005) 1181–1189.

[14] K. Liu and G. Coppola, Optimal design of damped dynamic vibration absorber for damped primary systems, *CSME Transaction* 34 (2010) 119-135.

[15] W. O. Wong and Y. L. Cheung, Optimal design of a damped dynamic vibration absorber for vibration control of structure excited by ground motion, *Engineering Structures* 30 (2008) 282–286.

[16] D.J. Inman, *Engineering Vibration*, 3rd Ed. Prentice Hall, Inc., Upper Saddle River, New Jersey, 2008.

Figure captions

Fig. 1. Schematic diagram of model A: a traditional dynamic vibration absorber (*m-k-c* system) attached to the primary (*M-K*) system.

Fig. 2. Schematic diagram of model B: the variant dynamic vibration absorber (*m-k-c* system) attached to the primary (*M-K*) system.

Fig. 3. Frequency response curve of the primary mass *M* of the traditional vibration absorber (Fig. 1) with $\mu = 0.1$ and $\gamma = 1$ at three different damping ratios.

Fig. 4. (a) Vibration amplitude of mass *M*, $|G_{\mathrm{A}}(\lambda_P)|$ and $|G_{\mathrm{A}}(\lambda_Q)|$ of the traditional DVA at the fixed points versus tuning ratio γ; (b) $\max_{\gamma,\zeta}\left(|G_{\mathrm{A}}(\lambda_P)|, |G_{\mathrm{A}}(\lambda_Q)|\right)$ versus tuning ratio γ. $\mu = 0.2$.

Fig. 5. Frequency response curve of the primary mass *M* of the non-traditional vibration absorber (Fig. 2) with $\mu = 0.1$ and $\gamma = 1$ at three different damping ratios.

Fig. 6. (a) Response amplitudes $|G_{\mathrm{B}}(\lambda_o)|$, $|G_{\mathrm{B}}(\lambda_P)|$ and $|G_{\mathrm{B}}(\lambda_Q)|$ of mass *M* of the non-traditional DVA (Fig. 2) versus tuning frequency γ; (b) $\max_{\gamma,\zeta}\left(|G_{\mathrm{B}}(\lambda_o)|, |G_{\mathrm{B}}(\lambda_P)|, |G_{\mathrm{B}}(\lambda_Q)|\right)$ versus tuning frequency γ with $\mu = 0.15$.

Fig. 7. (a) Response amplitudes $|G_{\mathrm{B}}(\lambda_o)|$, $|G_{\mathrm{B}}(\lambda_P)|$ and $|G_{\mathrm{B}}(\lambda_Q)|$ of mass *M* of the non-traditional DVA (Fig. 2) versus tuning frequency γ; (b) $\max_{\gamma,\zeta}\left(|G_{\mathrm{B}}(\lambda_0)|, |G_{\mathrm{B}}(\lambda_P)|, |G_{\mathrm{B}}(\lambda_Q)|\right)$ versus tuning frequency γ with $\mu = 2 - \sqrt{3}$.

Fig. 8. Frequency responses of the mass *M* of the non-traditional vibration absorber (Fig. 2) with $\mu = 0.2$.

Fig. 9. Schematic diagram of model C: a SDOF vibrating system with primary damping of damping coefficient *c* (*M-K-c*) system.

Fig. 10. Contours of $\dfrac{\left[\max(|G_{\mathrm{C}}(\lambda)|) - \max\left(|G_{\mathrm{B}}(\lambda, \mu, \gamma_{\mathrm{opt\_B}}, \zeta_{\mathrm{opt\_B}})|\right)\right]}{\max\left(|G_{\mathrm{C}}(\lambda, \zeta_{\mathrm{opt\_B}})|\right)}$ x 100% of the non-traditional vibration absorber.

Fig. 11. Contours of the resonant vibration amplitude $\max\left(|G_{\mathrm{B}}(\lambda, \mu, \gamma_{\mathrm{opt\_B}}, \zeta_{\mathrm{opt\_B}})|\right)$ of the non-traditional vibration absorber.

Fig. 12. Comparison of resonant vibration amplitudes $\max(|G_{\mathrm{B}}(\lambda)|)$ of the mass *M* of Model B at different mass ratio.

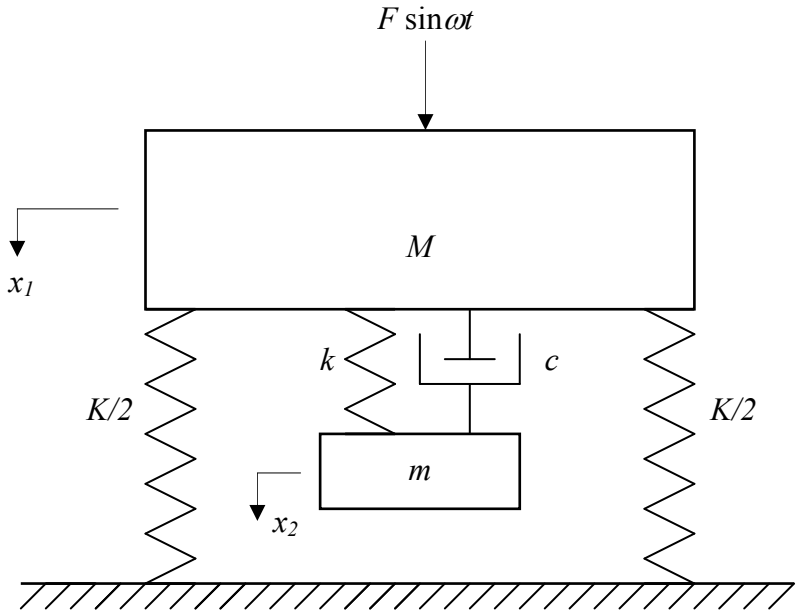

Fig. 1. Schematic diagram of model A: a traditional dynamic vibration absorber (*m*-*k*-*c* system) attached to the primary (*M*-*K*) system.

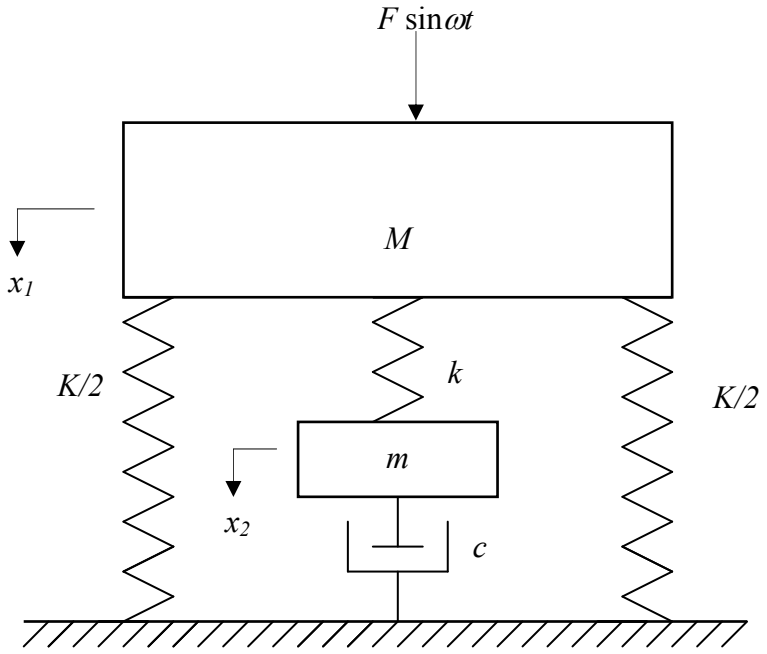

Fig. 2. Schematic diagram of model B: the variant dynamic vibration absorber (*m*-*k*-*c* system) attached to the primary (*M*-*K*) system.

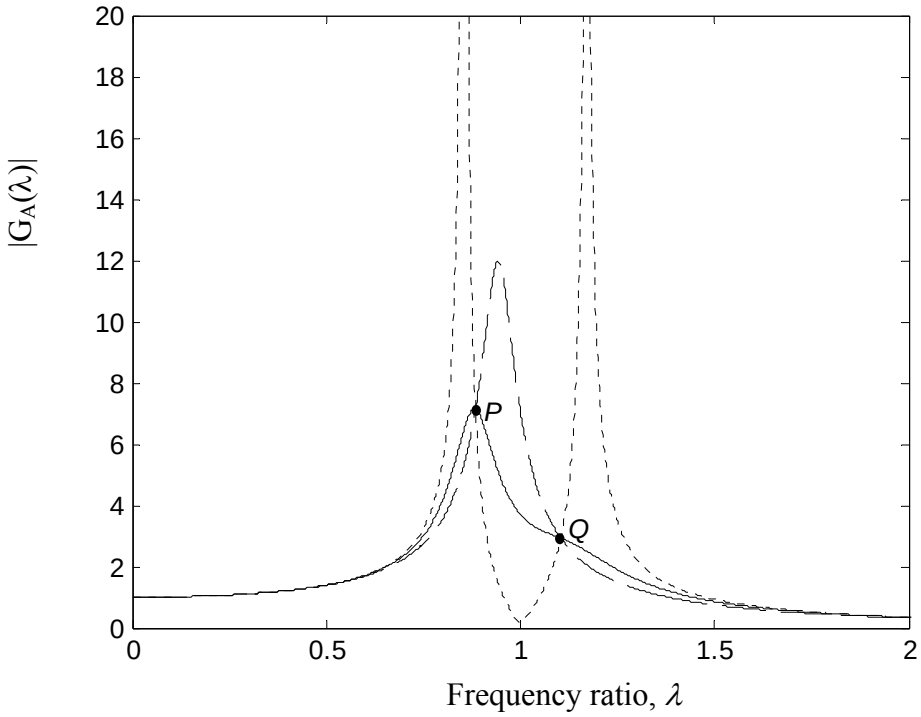

Fig. 3. Frequency response curve of the primary mass M of the traditional vibration absorber (Fig. 1) with $\mu = 0.1$ and $\gamma = 1$ at three different damping ratios.

------- $\zeta = 0.01$; – – – – – – $\zeta = 0.2$; ——— $\zeta = 0.5$.

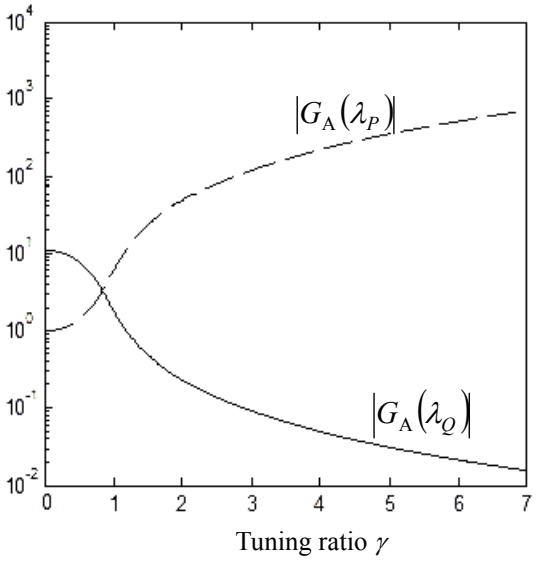

(a)

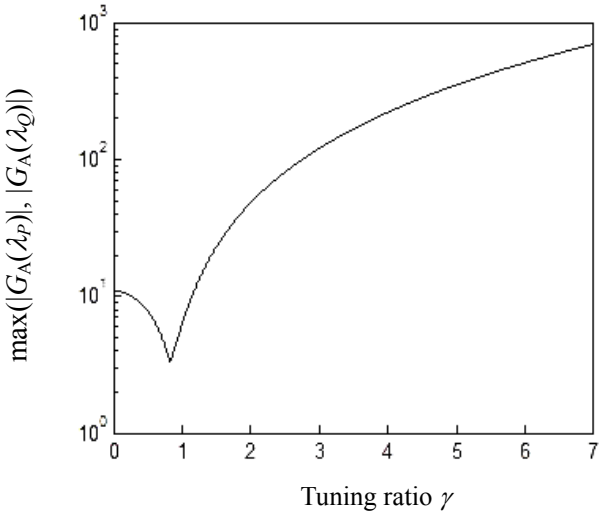

(b)

Fig. 4. (a) Vibration amplitude of mass M, $|G_A(\lambda_P)|$ and $|G_A(\lambda_Q)|$ of the traditional DVA at the fixed points versus tuning ratio γ; (b) $\max(|G_A(\lambda_P)|, |G_A(\lambda_Q)|)$ versus tuning ratio γ. $\mu = 0.2$.

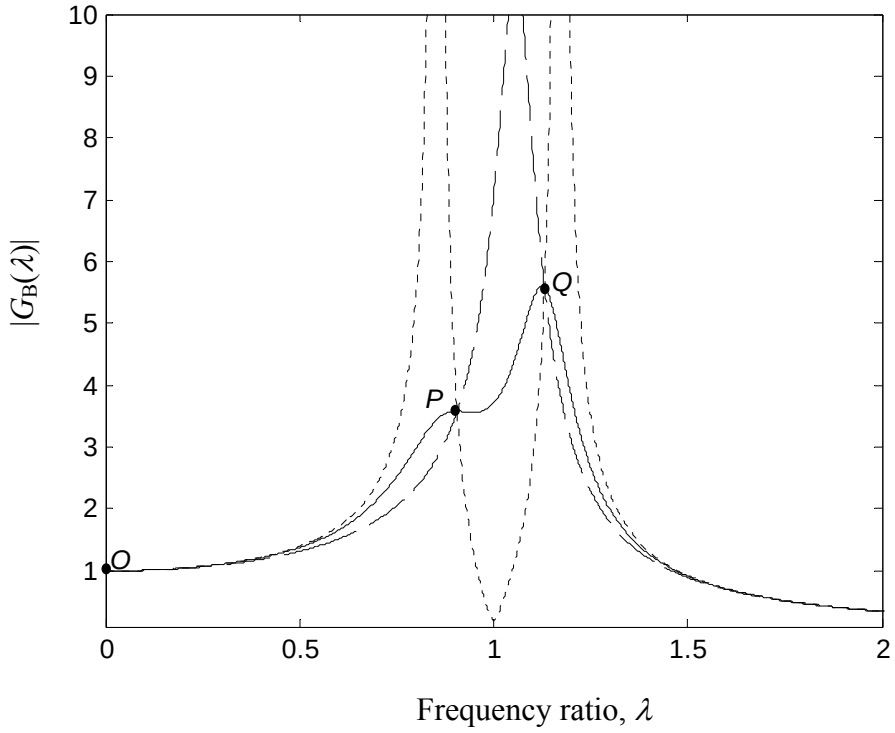

Fig. 5. Frequency response curve of the primary mass M of the non-traditional vibration absorber (Fig. 2) with $\mu = 0.1$ and $\gamma = 1$ at three different damping ratios.

------- $\zeta = 0.01$; – – – – – – $\zeta = 0.2$; ——— $\zeta = 0.5$.

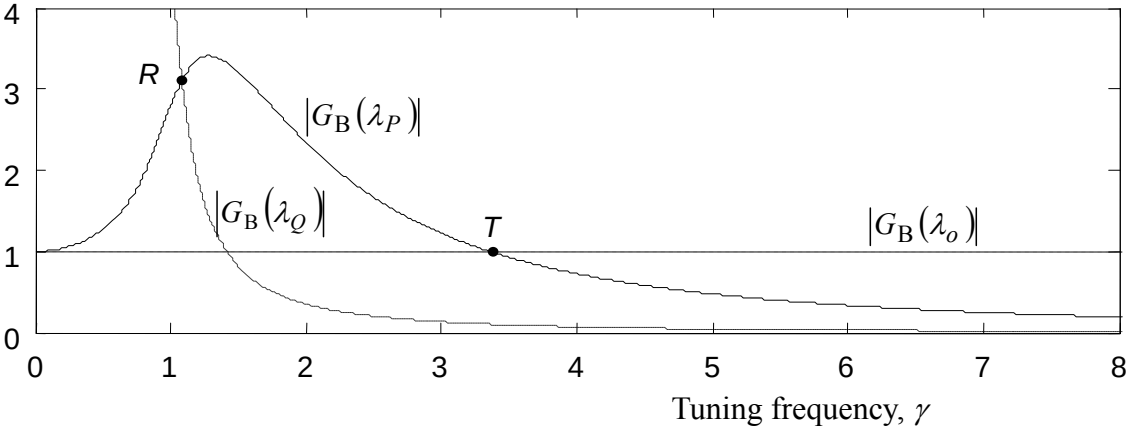

(a)

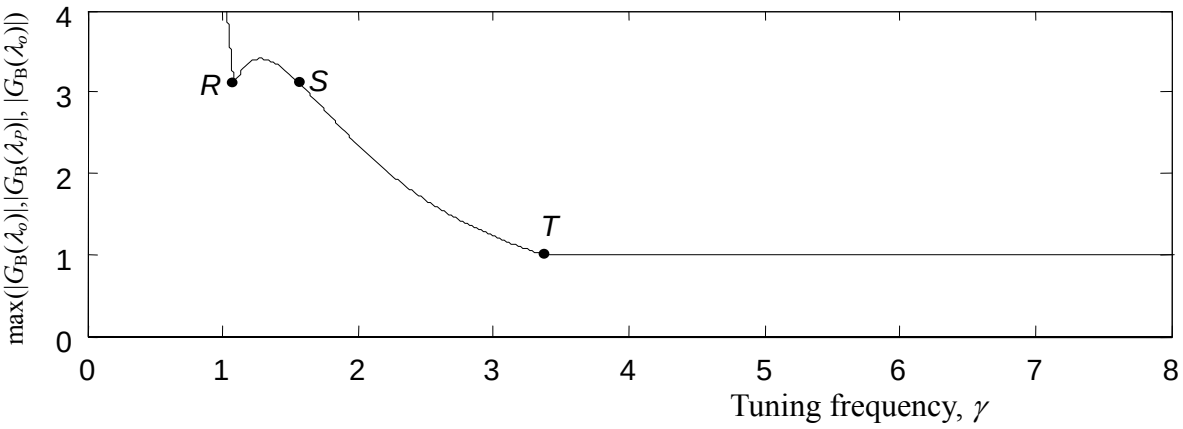

(b)

Fig. 6. (a) Response amplitudes $|G_{\mathrm{B}}(\lambda_o)|$, $|G_{\mathrm{B}}(\lambda_P)|$ and $|G_{\mathrm{B}}(\lambda_Q)|$ of mass M of the non-traditional DVA versus tuning frequency γ, (b) $\max_{\gamma,\zeta}\left(|G_{\mathrm{B}}(\lambda_0)|,|G_{\mathrm{B}}(\lambda_P)|,|G_{\mathrm{B}}(\lambda_Q)|\right)$ versus tuning frequency γ with $\mu = 0.15$.

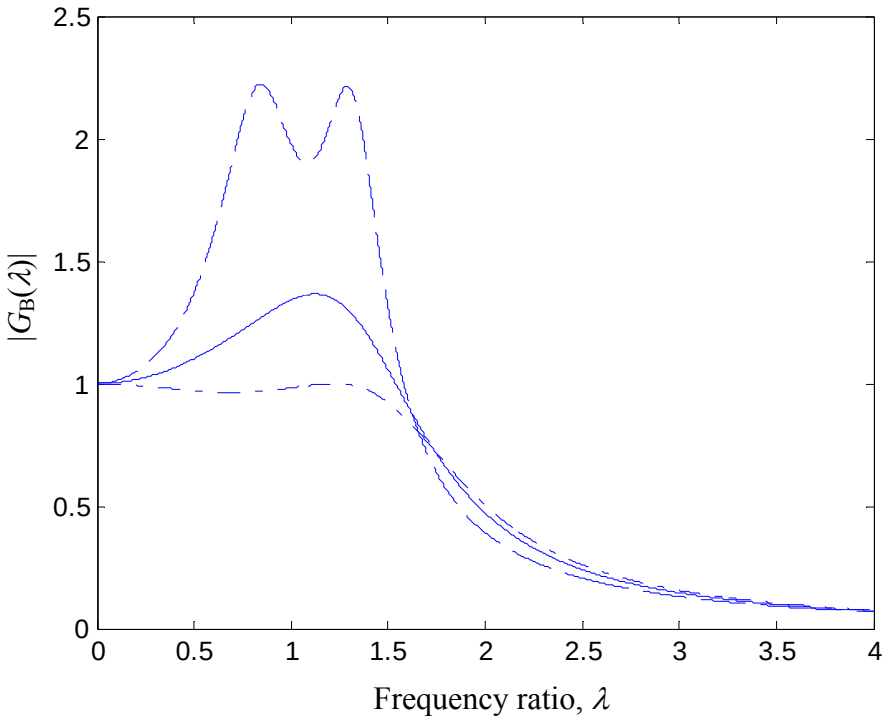

Fig. 8. Frequency responses of the mass M of the non-traditional vibration absorber (Fig. 2) with $\mu = 0.25$. ---------- Optimum tuning frequency γ_R from Eq. (20) and damping of absorber from Eq. (21) based on the fixed-points theory [12,13]; ——Optimum frequency $\gamma_{\text{opt\_B}} = 2$ and damping $\zeta_{\text{opt\_B}}$ from Eq. (29) of absorber; - · - · - · γ_T from Eq. (24) and damping $\zeta_T = \zeta_{\text{opt\_B}}\big|_{\gamma=\gamma_T}$ from Eq. (29) of absorber.

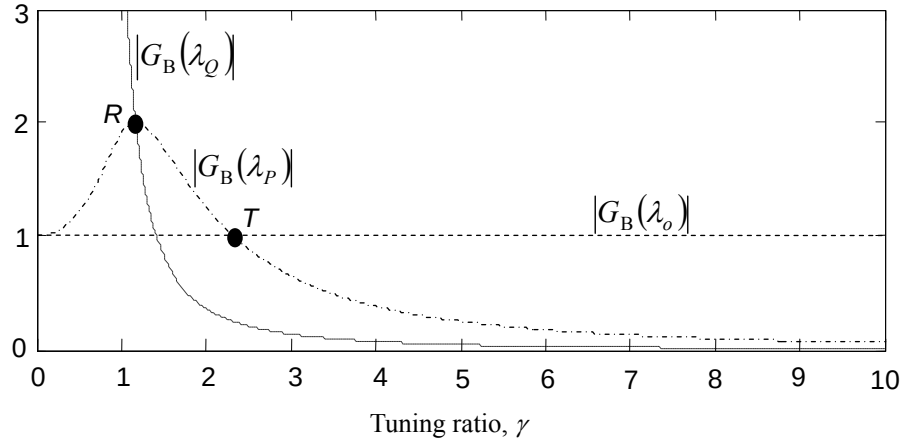

(a)

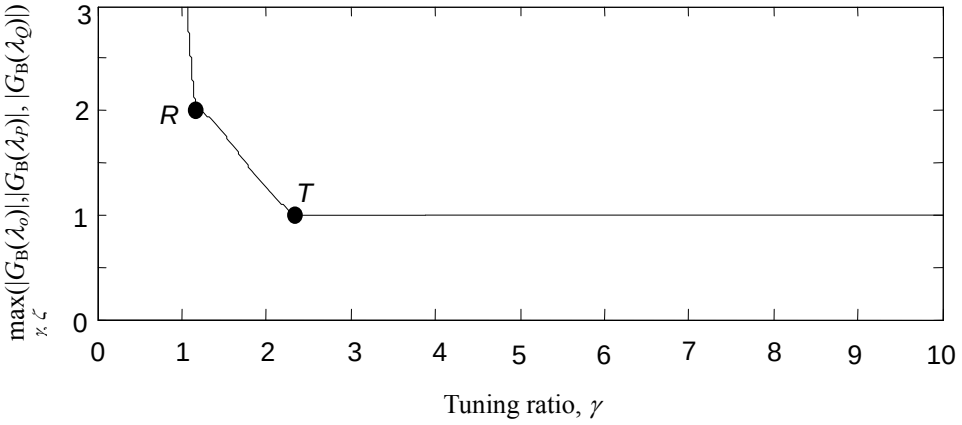

(b)

Fig. 7. (a)Response amplitudes $|G_B(\lambda_o)|$, $|G_B(\lambda_P)|$ and $|G_B(\lambda_Q)|$ of mass M of the non-traditional DVA versus tuning frequency γ, (b) $\max_{\gamma,\zeta}(|G_B(\lambda_0)|, |G_B(\lambda_P)|, |G_B(\lambda_Q)|)$ versus tuning frequency γ with $\mu = 2-\sqrt{3}$.

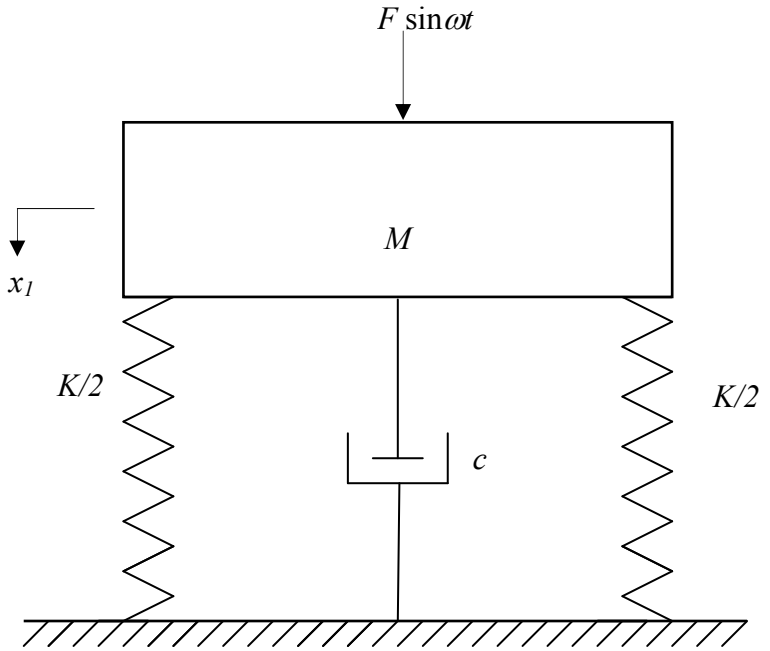

Fig. 9. Schematic diagram of model C: a SDOF vibrating system with primary damping of damping coefficient *c* (*M*-*K*-*c*) system.

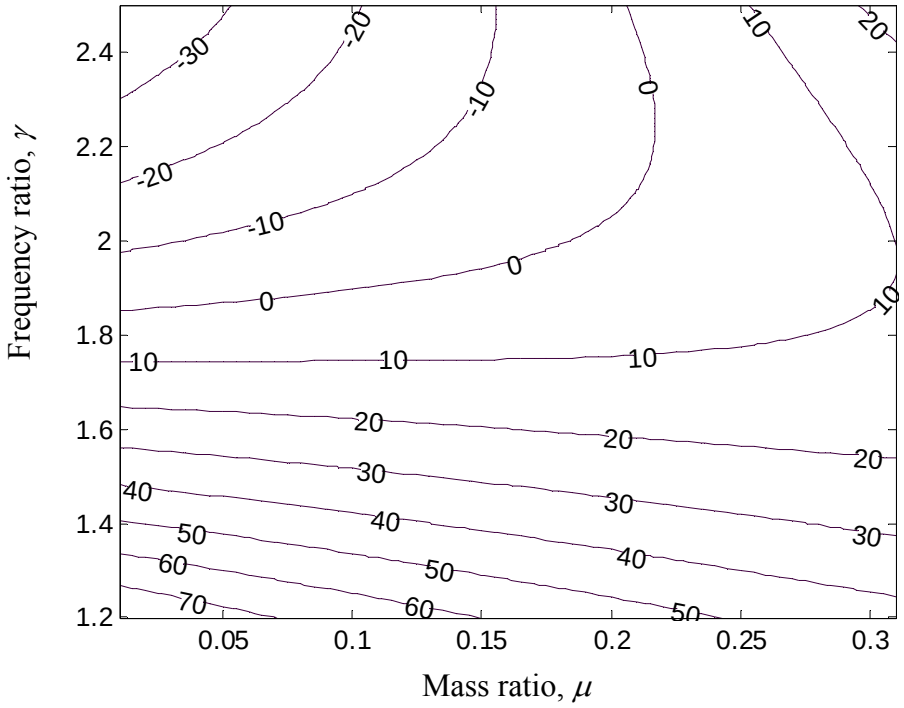

Fig. 10. Contours of $\dfrac{\left[\max(|G_{\mathrm{C}}(\lambda)|)-\max\left(\left|G_{\mathrm{B}}\left(\lambda,\mu,\gamma_{\mathrm{opt\_B}},\zeta_{\mathrm{opt\_B}}\right)\right|\right)\right]}{\max\left(\left|G_{\mathrm{C}}\left(\lambda,\zeta_{\mathrm{opt\_B}}\right)\right|\right)}$ x 100% of the non-traditional vibration absorber.

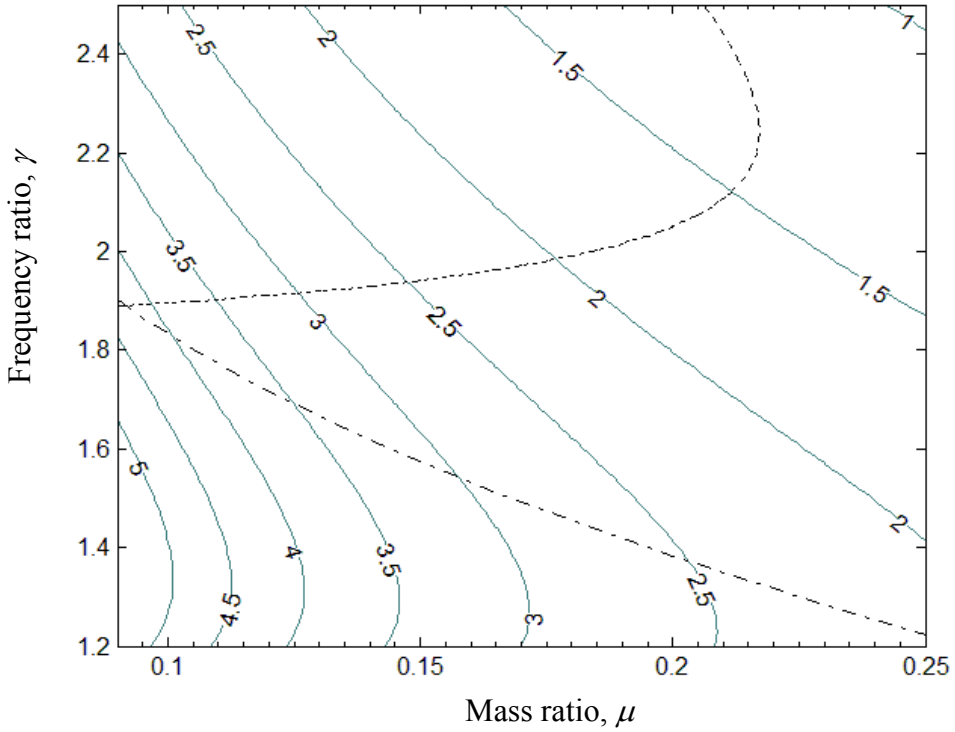

Fig. 11. Contours of the resonant vibration amplitude $\max\left(\left|G_{\mathrm{B}}\left(\lambda,\mu,\gamma_{\mathrm{opt\_B}},\zeta_{\mathrm{opt\_B}}\right)\right|\right)$ of the non-traditional vibration absorber. -·-·-·- Curve of γ_{S} (Eq. 23). ····· Curve of $\max(|G_{\mathrm{C}}(\lambda)|) = \max\left(\left|G_{\mathrm{B}}\left(\lambda,\mu,\gamma_{\mathrm{opt}},\zeta_{\mathrm{opt}}\right)\right|\right)$.

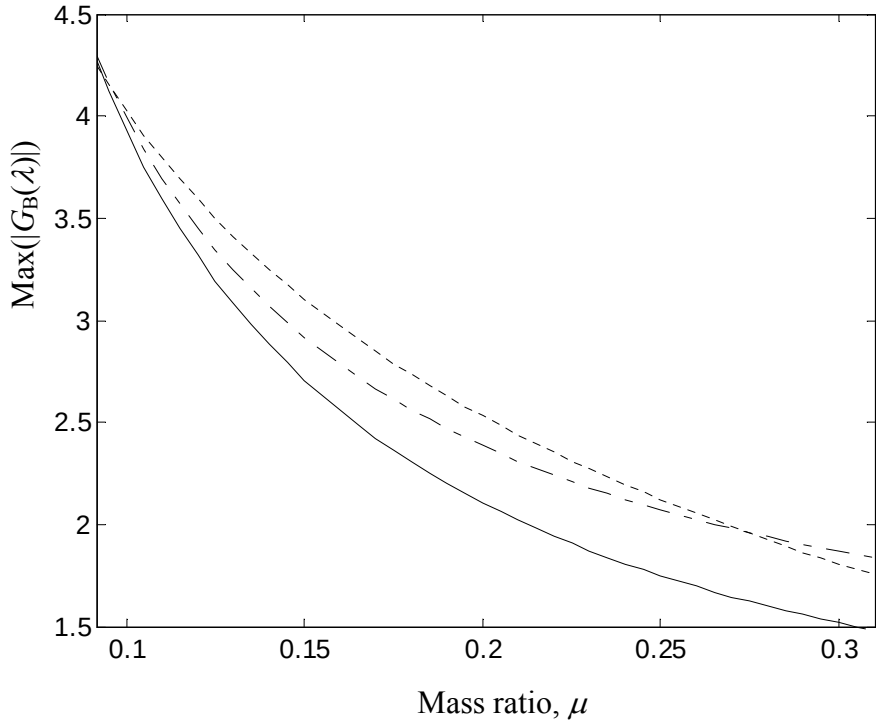

Fig. 12. Comparison of resonant vibration amplitudes $\max(|G_{\mathrm{B}}(\lambda)|)$ of the mass M of Model B at different mass ratio.

····· Using the optimum tuning parameters proposed in Refs. [12] and [13] Eq. (22), $\gamma = \gamma_R$ and $\zeta = \zeta_R$.

—— Using the proposed optimum tuning parameters $\gamma = \gamma_{\mathrm{opt\_B}}$ ($= 2.02 - 1.5\mu$) and $\zeta = \zeta_{\mathrm{opt\_B}}$.

-·-·- Using only the damper with the same damping coefficient (Fig. 9) for vibration suppression.